Interdisciplinary Description of Complex Systems 22(3), 246-265, 2024

A MODEL FOR AUTONOMOUS VEHICLE OBSTACLE AVOIDANCE AT HIGH SPEEDS

Dragan D. Stamenković* and Vladimir M. Popović

University of Belgrade, Faculty of Mechanical Engineering
Belgrade, Serbia

DOI: 10.7906/indecs.22.3.2
Regular article

Received: 21 May 2024.
Accepted: 15 June 2024.

ABSTRACT

The systems that are currently installed in autonomous vehicles are not designed to avoid obstacles on the road by manoeuvring at the limits of the vehicle and the road surface – the goal of the research presented was to develop such system. For these purposes, a universal test track based on ISO 3888-1 and ISO 3888-2 standards was adopted, which can be used to represent any situation in which there is an obstacle on the road in front of the vehicle that needs to be avoided. An analysis of the curves for generating the paths through the test track was carried out, on the basis of which the Bézier curves were chosen. In addition to them, the results of simulations in Adams Car software were used to generate the paths, which can be considered equivalent to real-world trials with a professional driver behind the wheel. A control model was developed for longitudinal and transverse control of the vehicle based on PID controllers, with the selection of optimal parameters – the ones that define PID controllers, and the others that define other characteristics of the model. The model proved to be successful in guiding the vehicle through the test track at all speeds at which manoeuvres are possible. Bézier curves are shown to be a better choice at lower speeds, while paths based on Adams Car simulations are a better choice at higher speeds.

KEY WORDS

autonomous vehicle, lateral control, double lane change, moose test, vehicle dynamics

CLASSIFICATION

ACM: I.6.0

JEL: R49

*Corresponding author, η: dstamenkovic@mas.bg.ac.rs; +381 63 656 254;
Kraljice Marije 16, 11120 Belgrade 35, Serbia

INTRODUCTION

The aim of the research presented in this article was to develop a model to control the autonomous vehicle in obstacle avoidance manoeuvres at high speeds. To the knowledge of the authors, there are no implemented systems that can guide the vehicle autonomously in a way to avoid the obstacle and safely return to the original lane at high speed at which stability of the vehicle can be impaired due to sharp manoeuvres.

To achieve this, co-simulations were conducted according to the scheme shown in Figure 1. Adams Car was used to create the vehicle model that will be controlled by the Simulink model (acting as a driver). In this co-simulation, Simulink is sending control inputs (steering wheel, throttle, brake, clutch and transmission) to Adams Car, while Adams Car is returning the data on vehicle dynamic behaviour (position, speed, acceleration…) to Simulink, which uses it to adapt the control signals.

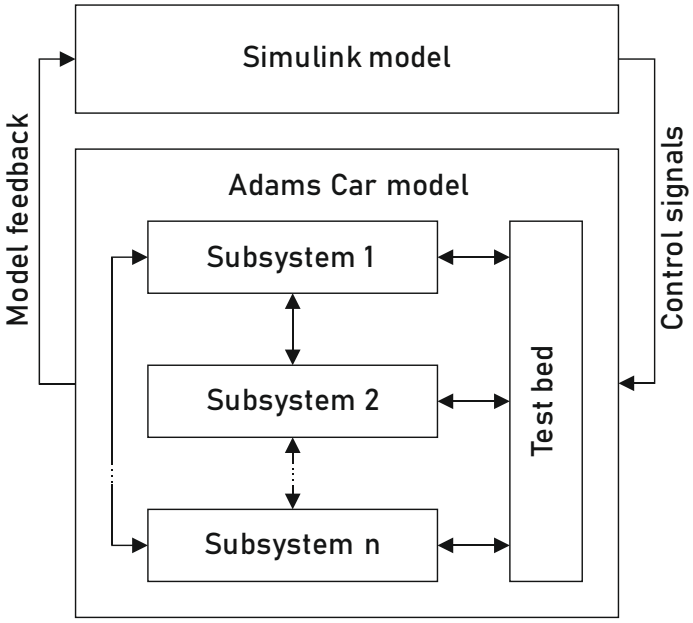

Figure 1. Co-simulation scheme.

To assess the stability and manoeuvrability of the vehicle, the tests described in the standards ISO 3888-1 (Double Lane Change Test) and ISO 3888-2 ("Moose" test) are used as a standard. These tests are carried out on the test track shown in Figure 2 and defined in Table 1.

Test 1 defined in ISO 3888-1 standard is performed by passing through the defined test track, where the recommended speed for entering section 1 is 80 ± 3 km/h, and during the test the position of the throttle should be kept in a constant position, as long as it is that possible.

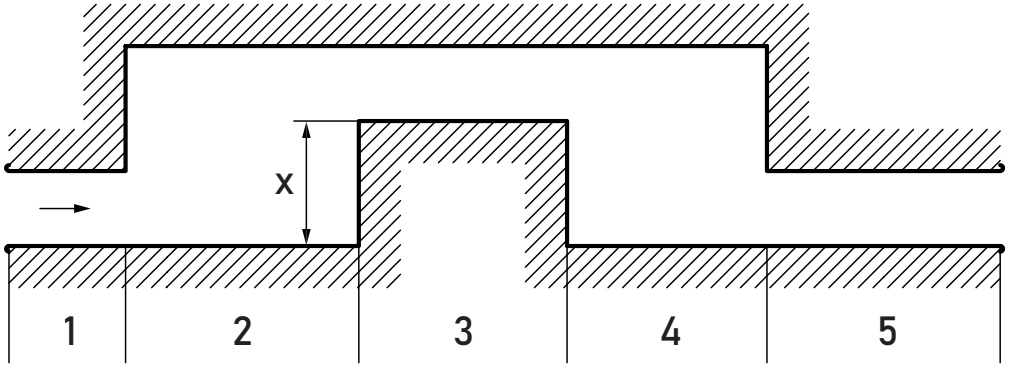

Figure 2. Test track according to ISO 3888-1 and ISO 3888-2.

When performing the "moose" test according to the ISO 3888-2 standard, section 1 is entered in the highest gear that provides at least 2 000 engine RPM. Two meters after entering section 1, it is necessary to release the throttle and cross the rest of the test track with it being released. All simulations done for the purpose of this research, regardless of test track dimensions, were performed at a constant speed.

Table 1. Test track dimensions according to ISO 3888-1 and ISO 3888-2 (b is vehicle width).

Section	Length, m		Width, m	
	ISO 3888-1	ISO 3888-2	ISO 3888-1	ISO 3888-2
1	15	12	$1{,}1b + 0{,}25$	
2	30	13,5		
3	25	11	$1{,}2b + 0{,}25$	$b + 1$
4	25	12,5		
5	30	12	$1{,}3b + 0{,}25$	$\min(1{,}3b + 0{,}25; 3)$
x			3,5	$1{,}1b + 1{,}25$

For the purpose of the research, an important assumption was made – every situation in which a vehicle has to change its lane to avoid an obstacle can be represented by the universal test track shown in Figure 3. The universal test track is based on the test tracks defined by ISO 3888-1 and ISO 3888-2 standards, and its dimensions depend on the data obtained using the sensors and cameras on-board the vehicle, for example like in [1].

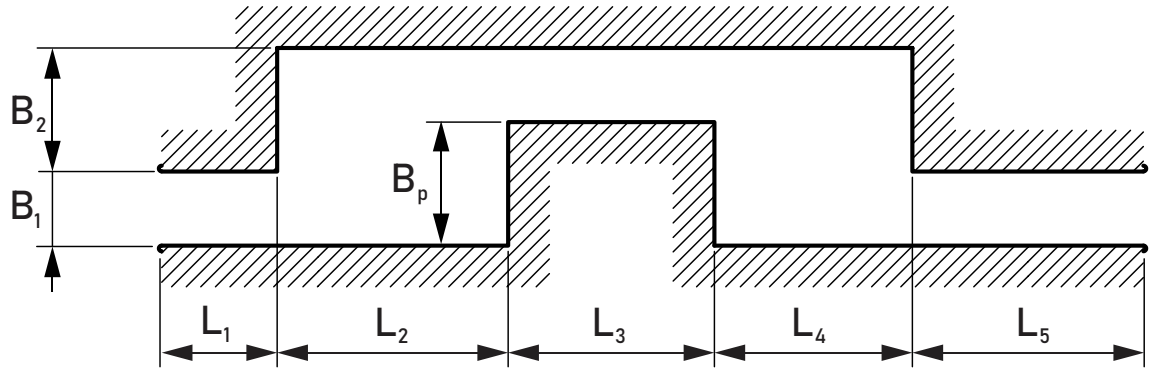

B_1	width of the ego vehicle's lane
B_2	width of the adjacent lane
B_p	length of the obstacle
L_1	projected distance between the ego vehicle and the vehicle in adjacent lane at the moment when ego vehicle enters the adjacent lane
L_1+L_2	distance between the vehicle and the obstacle
L_3	length of the obstacle
$L_2+L_3+L_4$	free length in the adjacent lane
L_4+L_5	free length in the original lane after the manoeuvre

Figure 3. Universal test track.

PATH DEFINITION

Next step was to choose the curve for path generation. Figure 4 shows eight different paths created by drawing eight different curves through or next to the defined points on the test track prescribed by the ISO 3888-1 using MATLAB functions listed in Table 2.

Table 2. Curves used to construct path.

Curve (with marks corresponding to Figure 3)		**MATLAB function**	**Additional parameter(s)**	**Lowest curve radius at ISO 3888-1 test track** [m]
a)	Cubic spline	`spline`	-	70
b)	Clamped cubic spline	`spline`	Starting and ending angles equal to zero	100
c)	Piecewise cubic Hermite interpolating polynomial	`pchip`	-	45
d)	Cubic smoothing spline	`csaps`	Smoothness factor: 0,01	115
e)	B-spline	`spmak`	Coefficients: 7; 7; 7 (three for 6^{th} order)	90
f)	B-spline (smoothing)	`spaps`	Tolerances: 0; 1; 1; 1; 1; 0	100
g)	3^{rd} order Bézier curve	[2]	-	70
h)	Modified Akima spline	`makima`	-	60

Of the eight curves shown, six are splines, and the seventh is a combination of two Bézier curves, so it can also be considered a spline, although it was not created by applying De Castelju's theorem. The points are chosen to be at the midpoint of the test track width at each point where the test track changes width, plus the start and the end of the test track. By moving the points towards the line that separates the two lanes (that is, towards the boundaries of the test track closer to this line), the curvature of the path would be reduced, which would allow the vehicle to pass at a higher speed, that is, reduce the probability of loss of lateral stability (in terms of skidding). Such a movement would require a sufficiently large test track section width and, presumably, increase the risk of the vehicle coming into contact with the boundaries of the test track.

It can be concluded that cubic spline, smoothing B-spline and modified Akima spline are not suitable for constructing the path, since the tangent to these curves at the initial points does not coincide with the vehicle velocity vector. B-spline and cubic smoothing spline also proved to be inappropriate, the reason being their deviation from the first defined point (where the vehicle is at the beginning of the test track). Piecewise cubic Hermite interpolating polynomial is characterized by high curvature values, which also makes it unsuitable for constructing the path. Although by looking at figure 4 one might conclude that clamped cubic spline is suitable for constructing the path, it would require the vehicle to steer to the opposite direction from the direction of the lane change, before the change itself, which will consume already deficient time.

According to the analysis conducted, the path was constructed in two ways – using Bézier curves and based on paths generated by independent Adams Car simulations. Paths generated by independent Adams Car simulations can be considered as being the paths "recorded" during manoeuvres performed by a trained professional driver, and therefore desirable for passing through the test track.

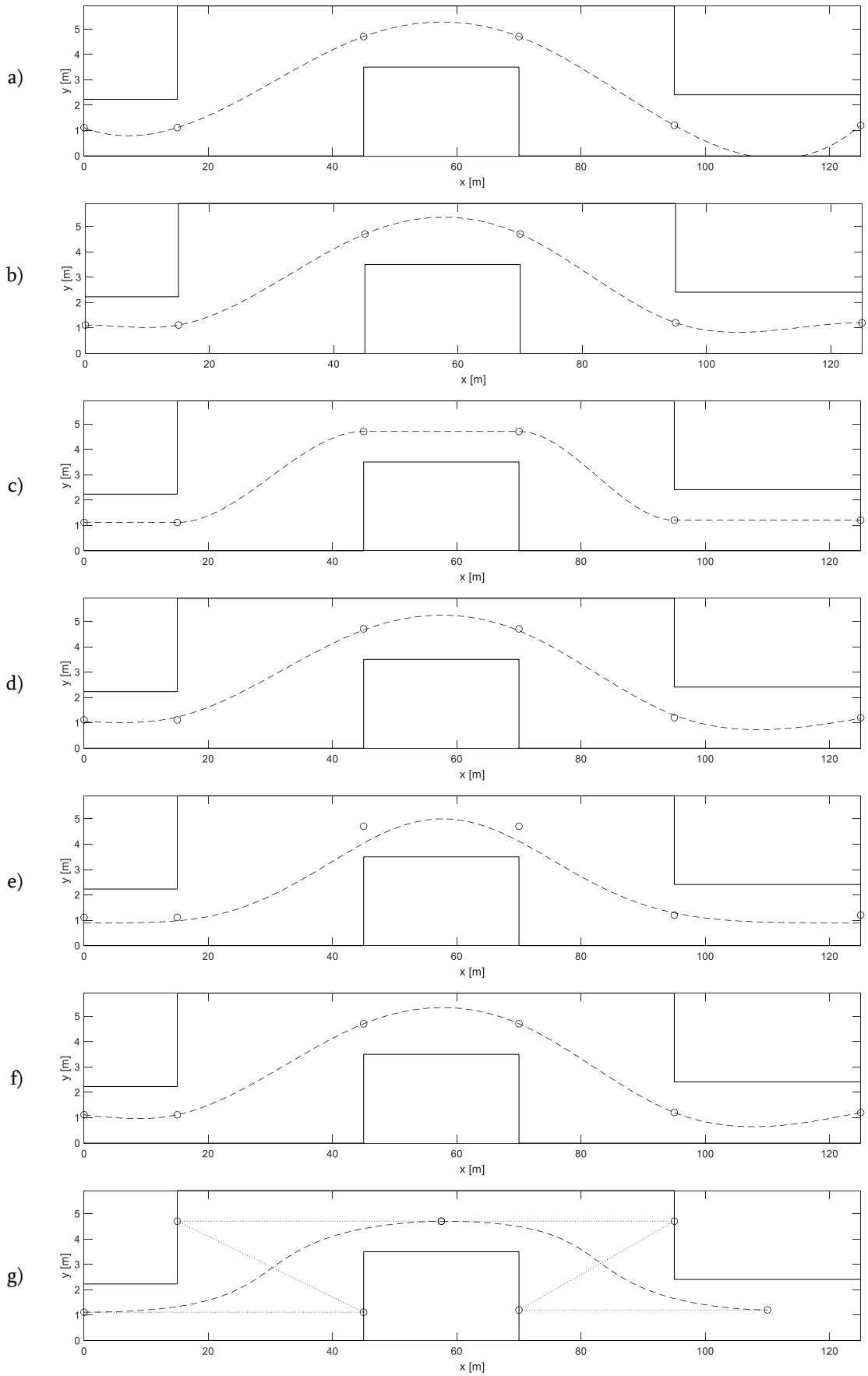

Figure 4. Path construction.

LATERAL CONTROLLER

There are many strategies used to control the autonomous vehicle [3]. Longitudinal control of the vehicle (controlling the vehicle speed by controlling the engine, transmission and brakes) was established relatively easily by using PID controller. On the contrary, lateral vehicle control proved to be a much greater challenge. Controlling a steering system during manoeuvres at the limit of a vehicle's capabilities presents a very different challenge compared to the control of robots moving at low speeds (which can be read about in [4]).

According to [5], heuristic methods reduce the complexity of the problem by simplifying the shapes of objects and limiting the movement of vehicles to smaller sets. However, most methods generate paths rather than trajectories. That's why geometric methods are suitable mainly for applications at low speeds (in automatic parking, for example).

Most of the controllers shown in the literature are successful in following traffic lanes or vehicles in front on the highway (where the curve radii are large, without the need for sudden manoeuvres) [6], especially those that make steering wheel angles directly dependant on the desired change in yaw angle (for low values) [7], where the desired change in the yaw angle is defined in advance for a given manoeuvre. The proportional regulator was also used in the famous ARGO project [8].

The human vehicle control process consists of three submodels: target path planning, feed-forward, and feedback [9], and the same applies when the vehicle is controlled by the computer. Steering feedback is used to form a control signal based on monitored parameters (vehicle speed and curvature of the road ahead, for example), while the task of feedback is to correct the control signal based on deviations from the desired behaviour (desired path, for example)

PID controllers are often constructed based on simplified models of vehicle behaviour, taking into account that the actual behaviour of the vehicle differs from that predicted by the geometric model (due to steering, vehicle inertia...) [8]. Some authors believe that the use of PID controllers for lateral vehicle control is difficult because determining the optimal coefficients is a big challenge [10], and they cannot be constant – they must depend on the current state of the vehicle (for example, in [11] it is stated that the coefficient K_p must increase with increasing curvature of the desired path, in order to allow a faster dynamic response, while lower values on a straight path ensure stability at higher speeds). This may be supported by the fact that in [12] the PID controller for the throttle is precisely described and defined, while no details are given about the controller responsible for turning the steering wheel, although the authors claim that it was successfully implemented.

In the 1960s, in Japan, a controller was used for lateral vehicle control with control signal representing the sum of the signal calculated by the PD controller based on the deviation from the path and the signal calculated by the proportional controller based on the yaw angle error [8].

The "Stanley" method, used to control the vehicle of the same name, is a nonlinear feedback loop based on kinematics as a function of deviation from the desired path (lateral deviation and yaw angle). The performance of this method drops sharply at higher speeds [13]. Similarly, "Sandstorm", the vehicle that participated in same competitions (DARPA Grand Challenges in 2004 and 2005) used a simple control model based on kinematics. On the opposite side, "Boss", the winner of the "DARPA Urban Challenge 2007" competition, used a much more advanced system based on model predictive control [8].

The results of several studies also show that lateral control of the vehicle is a big challenge. In the first of them, the vehicle was controlled based on model predictive control for double lane change. At a speed of 7 m/s, the vehicle was able to successfully follow the set path, while at higher speeds this was not the case [14].

Recorded deviations from the desired path in lane change along 20 m (longitudinal distance from the planned start to the planned end of the manoeuvre) at a speed of 20 m/s using different models from the literature obtained by the authors in a study described in [15] also add to the conclusion about the complexity of the problem.

Table 3 shows an overview of the methods used for lateral vehicle control [8] – the optimal (according to the authors of the review) application of these methods does not include the manoeuvres that are the subject of this article.

Table 3. Review of methods used for lateral vehicle control [8].

Method		Suitable use
Geometric and kinematic models	Simple pursuit for the point on the desired path	Slow driving
	"Stanley"	Smooth highway driving / parking manoeuvres
	Kinematic chain model	Smooth parking manoeuvres
Feed-forward linear-quadratic regulator		Smooth urban driving at higher speeds
Forward-looking linear-quadratic regulator		Highway driving at relatively constant speed

The starting model was an open-loop model, based on [16], where the control signal (steering wheel position) is directly proportional to the desired yaw rate, which is known from previously conducted stand-alone Adams Car simulations. The proportionality coefficient depends on the speed of the vehicle (for 10 m/s K_p = 0.105, for 20 m/s K_p = 0.06). Unlike the model given in [16], the sideslip angle of the vehicle was not used to generate the steering signal – it was shown to have no effect on the relationship between the desired steering wheel angle and the yaw rate of the vehicle. The disadvantage of this model is that there is no feedback and no way to generate a reference dependence of the yaw rate on time for every possible combination of vehicle speed and test track dimension. Therefore, a feedback model was developed, that forms the steering signal (desired yaw rate, i.e. steering wheel angle) based on the deviation from the y coordinate, after which it corrects it based on the difference between the desired and actual yaw rate, as was done in [17]. The problem with this model is that it works only at lower speeds while already at a speed of 20 m/s on ISO 3888-1 test track the vehicle loses stability. The loss of the stability occurs because the model requires excessive steering wheel angles to correct the deviation from the y coordinate. The model does not take into account the angle of the vehicle with respect to the tangent to the path at the reference point (which is important, as stated in [18]), and moreover it reacts late – only when the deviation has occurred, not in advance, as a human would do. For this reason, it was decided to steer the vehicle based on the projected deviation from the desired path y_g, which is observed at a distance l_u in front of the front axle of the vehicle, which is defined as the product of the vehicle's longitudinal speed and time t_p. Some of the recommendations that can be found in the literature for determining the look-ahead point (the point at which a deviation from the desired path is observed on the basis of which the control signals are generated), through the time needed for vehicle to reach the given point or by the distance from the vehicle to that point are:

- time of 1 s [19],
- time of 1.4 s for 72 km/h [10],
- distance of $l_p + l_u$ = 12 m [17],
- the distance must depend on the speed of the vehicle [20],
- the distance must be a quadratic function of the vehicle speed [21].

Just as it is difficult to imagine that a human would use only one point seen through the windshield to make an appropriate decision, so it is difficult to expect a control unit to make the correct decision based only on a deviation in one point [12]. Therefore, some researchers suggest for the projected deviation to be monitored in a larger number of points in front of the vehicle [9, 22, 23]. The control signal can also be generated based on weighted distances from the desired path [9, 19]. This approach was also tried, but ran into problems when the vehicle was in a situation where these deviations were not of the same sign – then these deviations would work against each other (the vehicle would steer on the basis of deviations with one sign, which would further increase deviations of different sign and thus create a "vicious circle" of vehicle yaw).

Therefore, it was decided to use the distance at only one point in front of the vehicle to generate the signal. It is very important to make a correct choice of the distance at which the distance from the desired path is determined – if it is too far in front of the vehicle, it is not suitable to act on the basis of the information at the moment of its receipt, and the information will be lost by the time it can be useful; if it is too close to the vehicle, it will cause poor steering (the model will resemble a model operating based on instantaneous deviation), especially at higher speeds [12].

The final model, based on [17], is shown in Figure 5. The differences introduced in relation to the model on which it was based are as follows:

- the modified model includes only proportional regulators, which simplifies it,
- the coefficients are variable and depend on the speed and dimensions of the test track,
- a correction was introduced due to the responsiveness of the system (the original model was intended for gentler manoeuvres) – x_k.

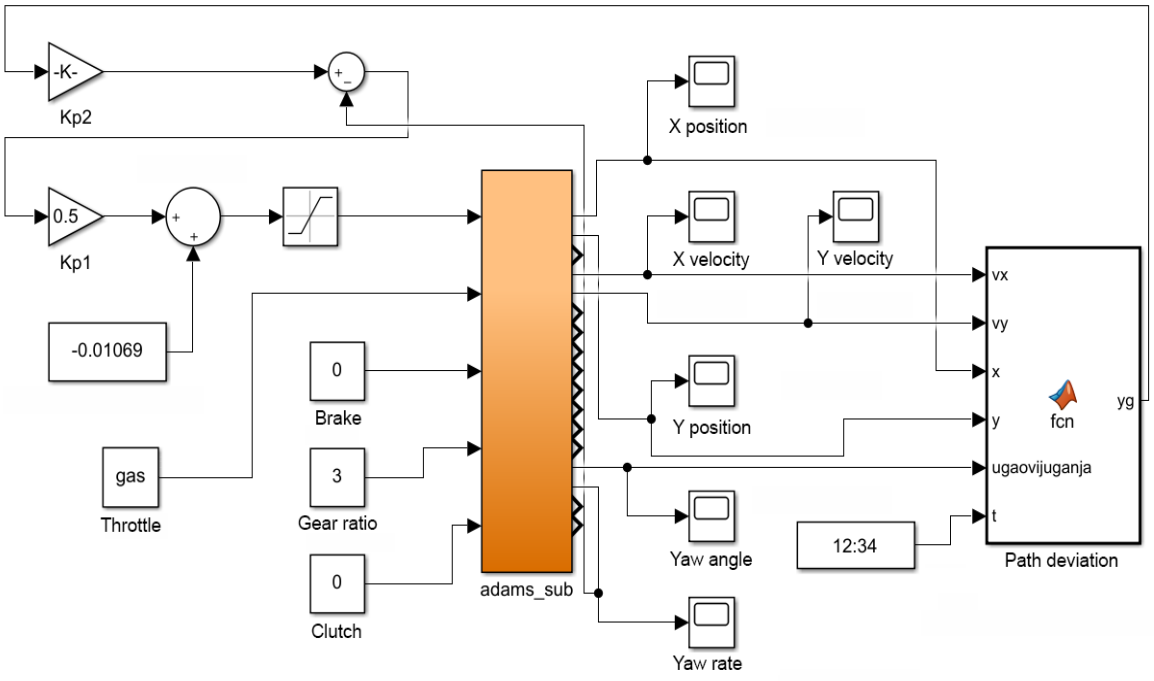

Figure 5. Final controller.

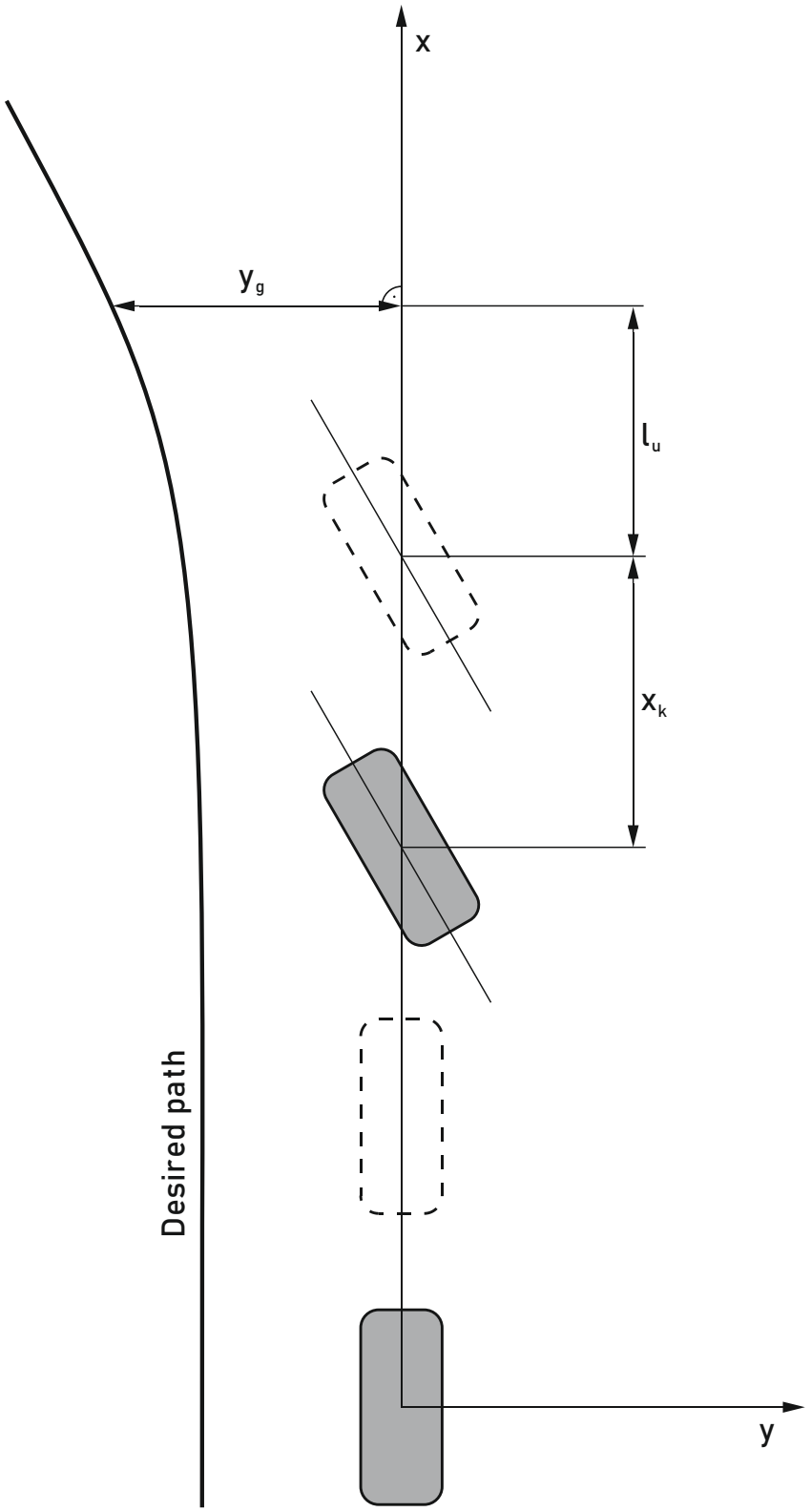

Figure 6. Projected lateral path deviation with latency correction.

RESULTS

Simulations were conducted for the test tracks according to ISO 3888-1, ISO 3888-2 and also for the test track #3, constructed as a track with the dimensions being in between the dimensions of the first two. They were done for the speeds up to maximum values that does not lead to the loss of the stability. The results for those maximum speed values are shown in Table 4.

Table 4. Simulation results (continuation on pp.256-260).

Manoeuvre	**ISO 3888-1 35 m/s**
Path	Bézier
K_{p1}	0,8
K_{p2}	0,01
t_p [s]	0,31
x_k [m]	11

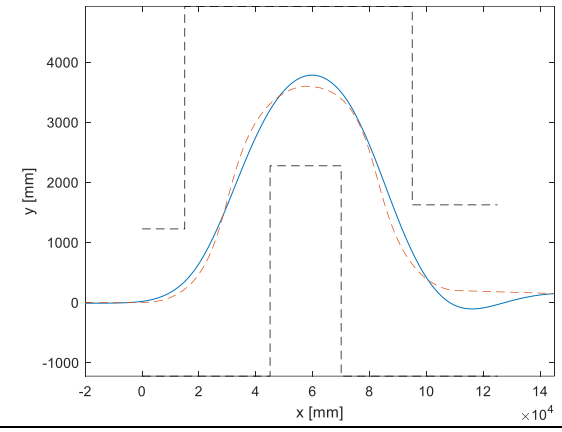

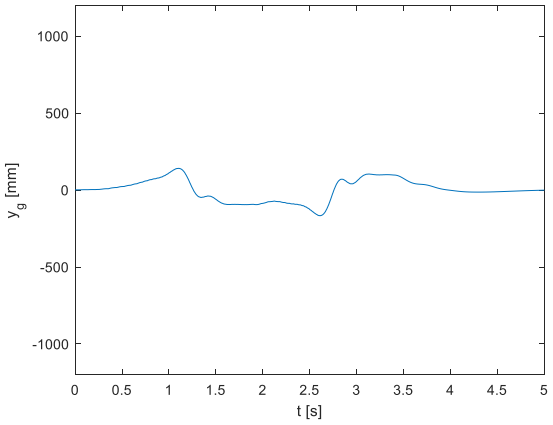

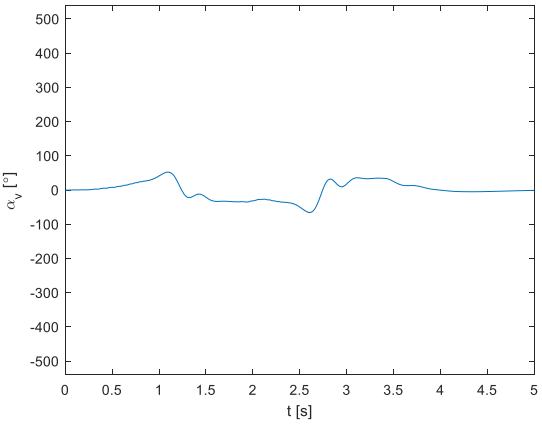

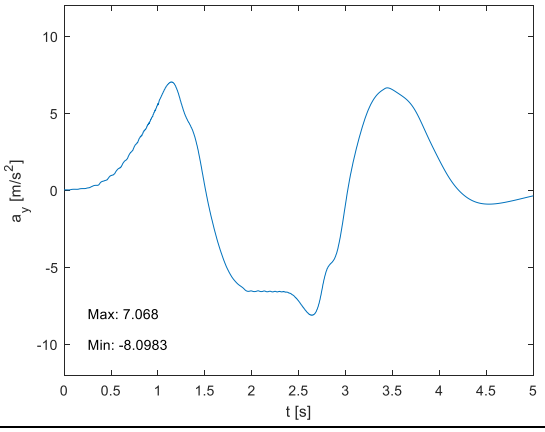

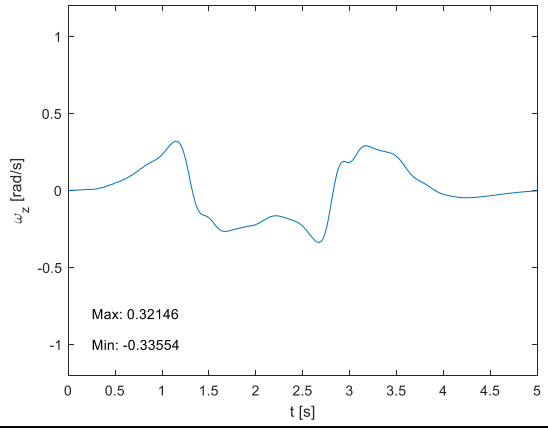

- - – desired
— – obtained
x – longitudinal vehicle position
y – lateral vehicle position
t – time
y_g – projected path deviation
α_v – steering wheel angle
a_y – lateral acceleration
ω_z – yaw rate

Table 4. Simulation results (continued from p.255, continuation on pp.257-260).

Manoeuvre	**ISO 3888-1 35 m/s**
Path	*Adams Car*
K_{p1}	0,8
K_{p2}	0,01
t_p [s]	0,34
x_k [m]	12

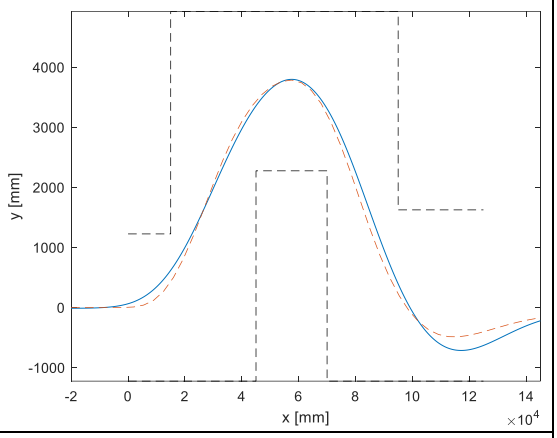

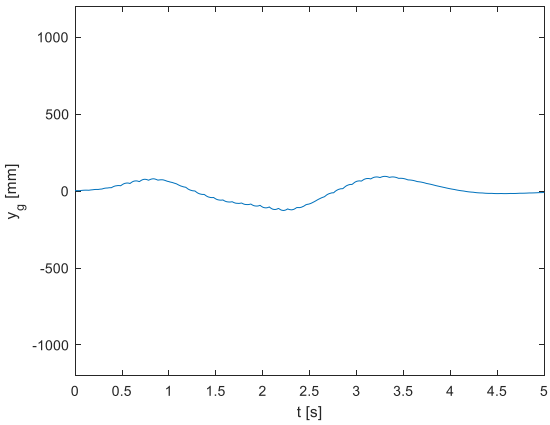

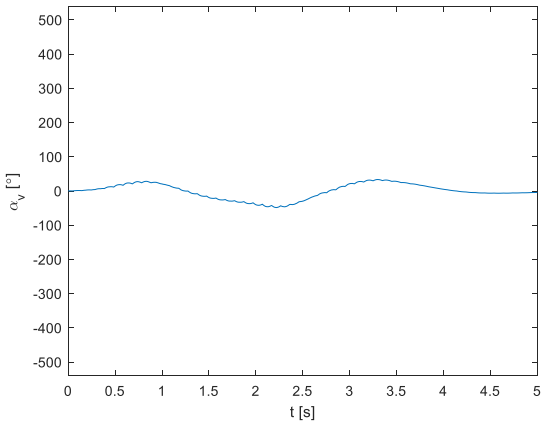

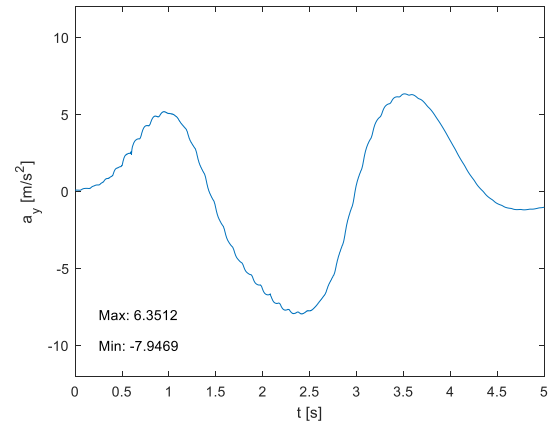

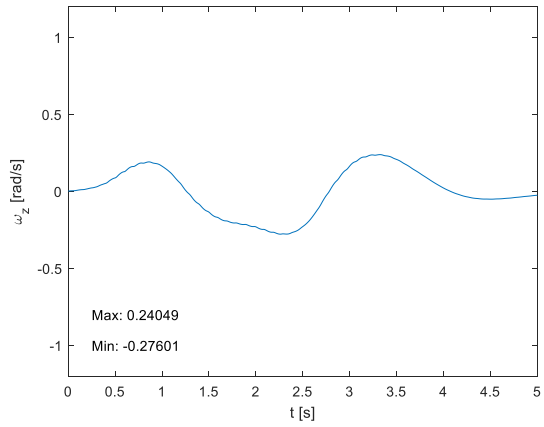

- – – desired
- —— obtained
- x – longitudinal vehicle position
- y – lateral vehicle position
- t – time
- y_g – projected path deviation
- α_v – steering wheel angle
- a_y – lateral acceleration
- ω_z – yaw rate

Table 4. Simulation results (continued from pp.255-256, continuation on pp.258-260).

Manoeuvre	**#3 30 m/s**
Path	Bézier
K_{p1}	0,8
K_{p2}	0,01
t_p [s]	0,31
x_k [m]	7,5

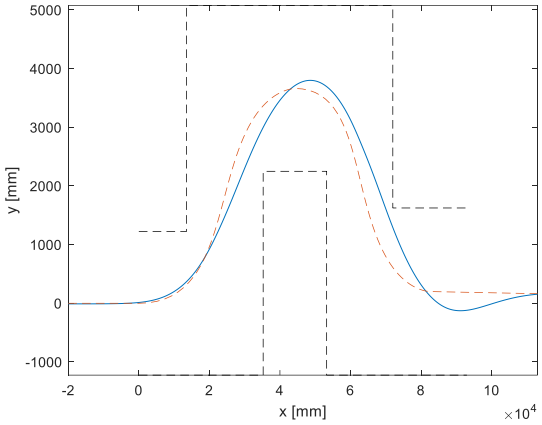

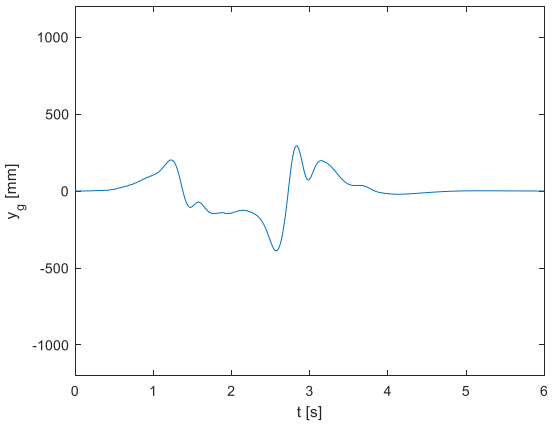

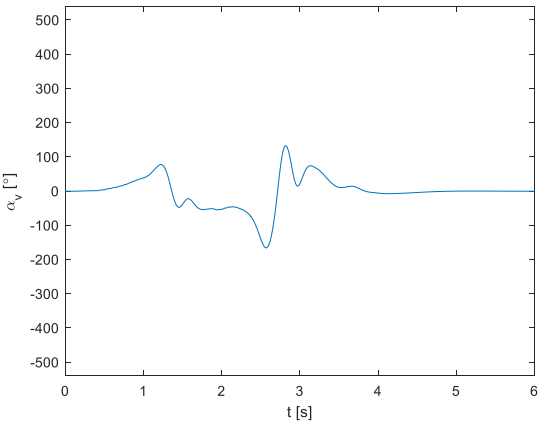

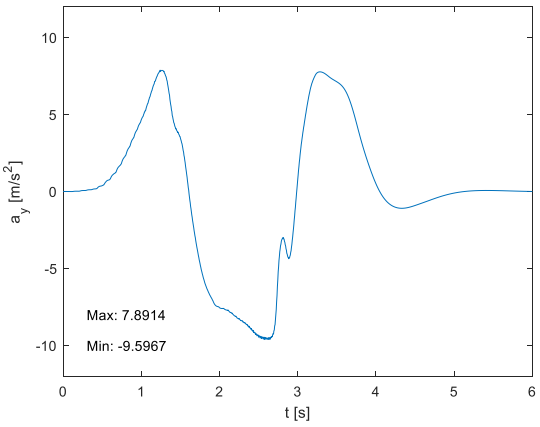

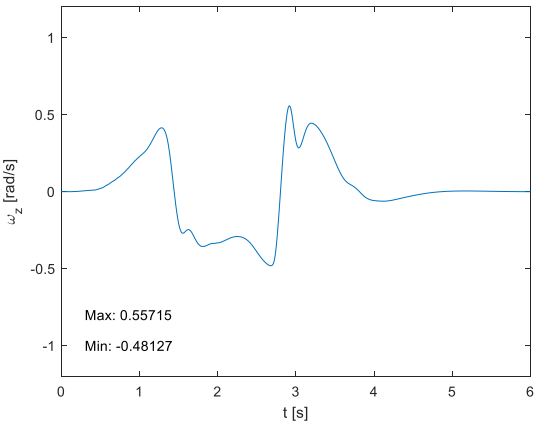

- - – desired
— – obtained
x – longitudinal vehicle position
y – lateral vehicle position
t – time
y_g – projected path deviation
α_v – steering wheel angle
a_y – lateral acceleration
ω_z – yaw rate

Table 4. Simulation results (continued from pp.255-257, continuation on pp.259-260).

Manoeuvre	**#3 30 m/s**
Path	*Adams Car*
K_{p1}	0,8
K_{p2}	0,01
t_p [s]	0,35
x_k [m]	8,5

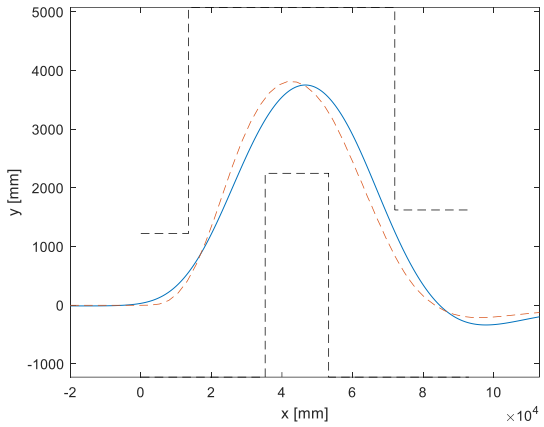

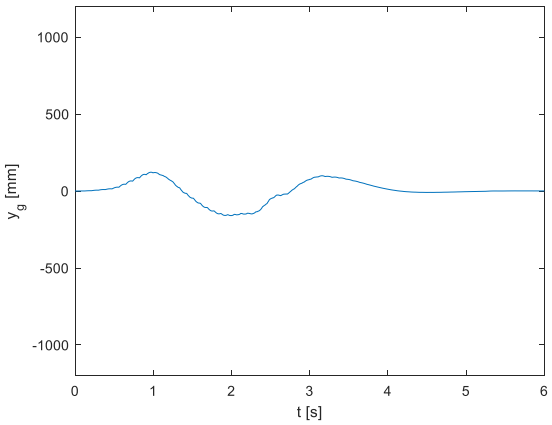

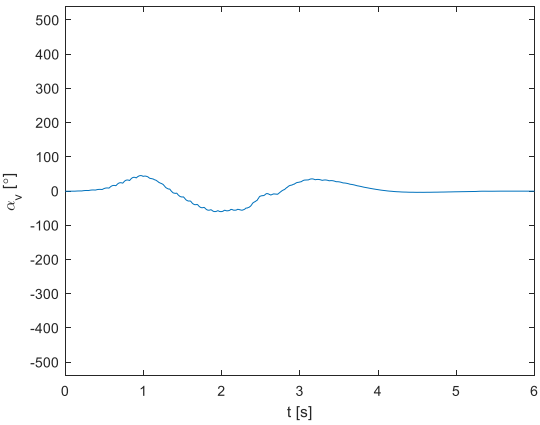

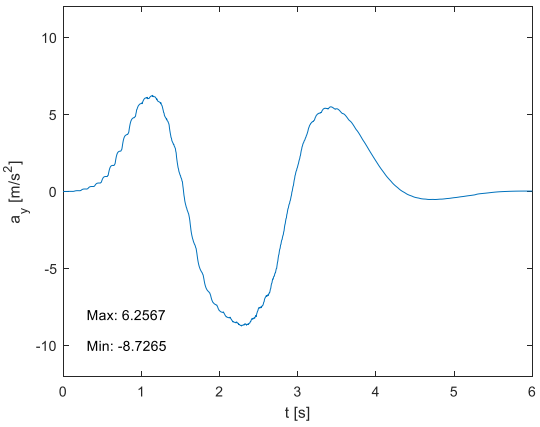

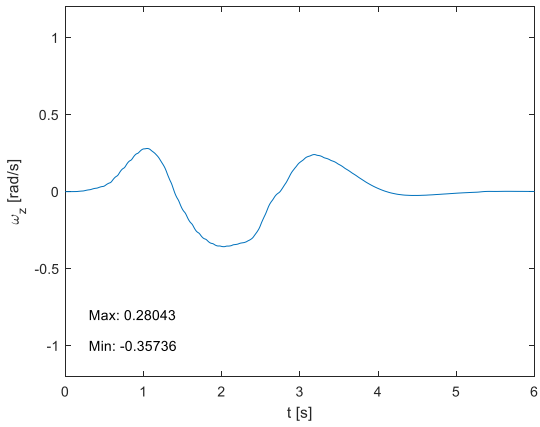

- - – desired
— – obtained
x – longitudinal vehicle position
y – lateral vehicle position
t – time
y_g – projected path deviation
α_v – steering wheel angle
a_y – lateral acceleration
ω_z – yaw rate

Table 4. Simulation results (continued from pp.255-258, continuation on p.260).

Manoeuvre	**ISO 3888-2 20 m/s**
Path	Bézier
K_{p1}	0,9
K_{p2}	0,01
t_p [s]	0,3
x_k [m]	6

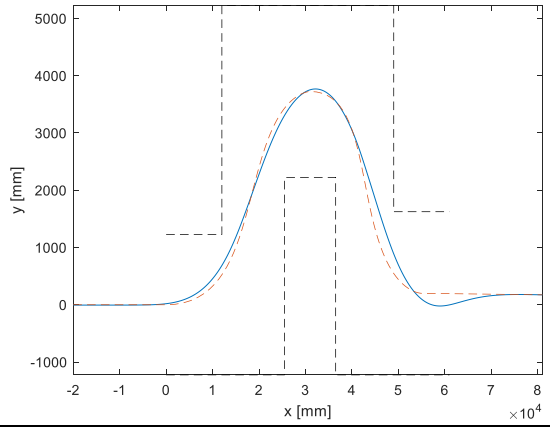

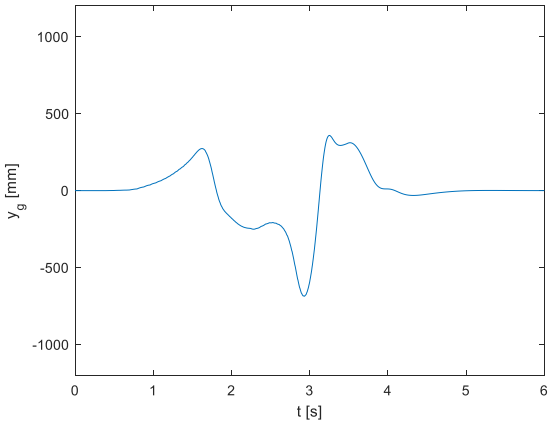

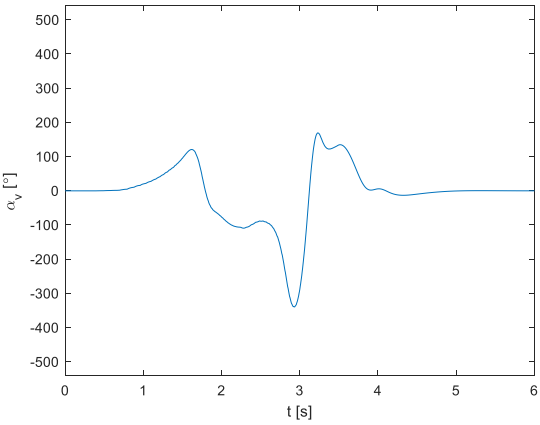

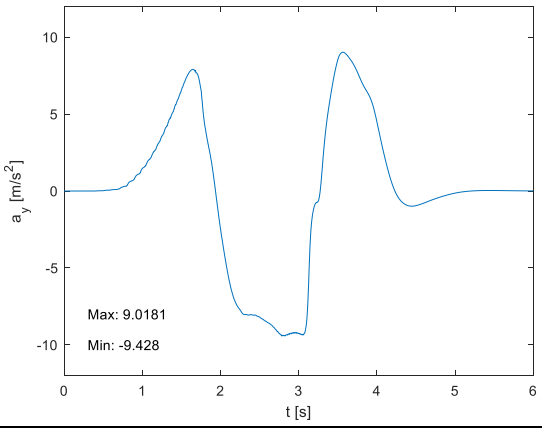

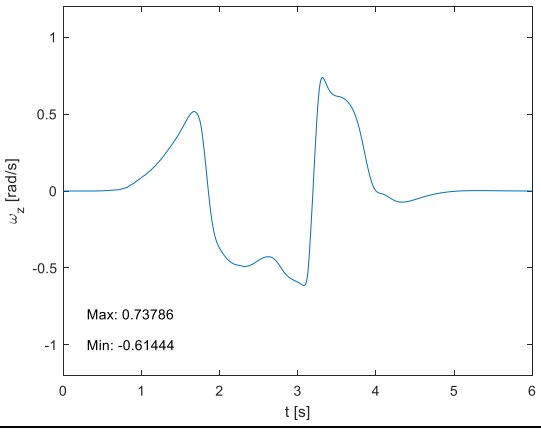

- - – desired
— – obtained
x – longitudinal vehicle position
y – lateral vehicle position
t – time
y_g – projected path deviation
α_v – steering wheel angle
a_y – lateral acceleration
ω_z – yaw rate

Table 4. Simulation results (continued from pp.255-259).

Manoeuvre	**ISO 3888-2 20 m/s**
Path	*Adams Car*
K_{p1}	0,9
K_{p2}	0,01
t_p [s]	0,35
x_k [m]	7

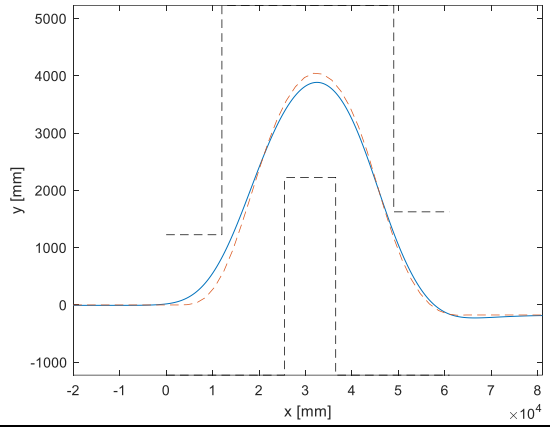

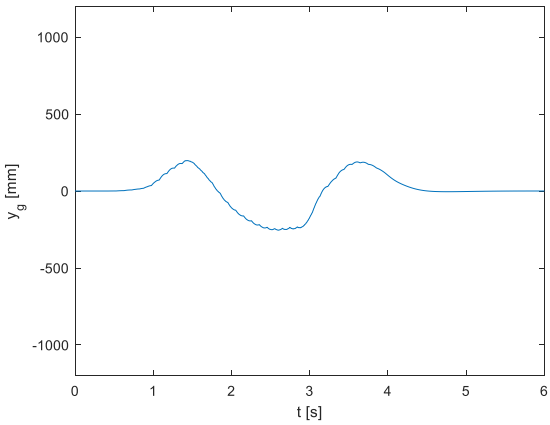

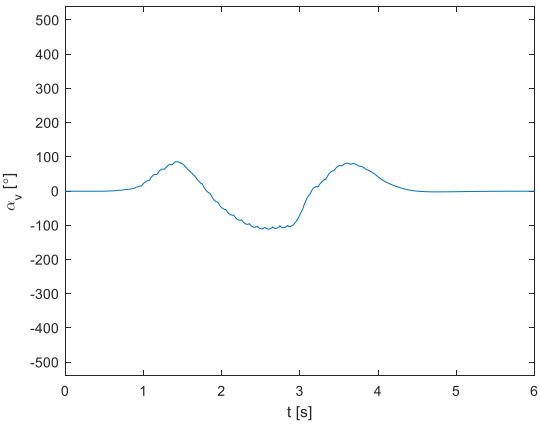

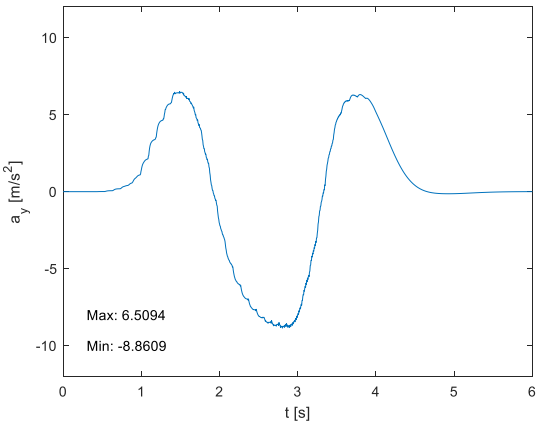

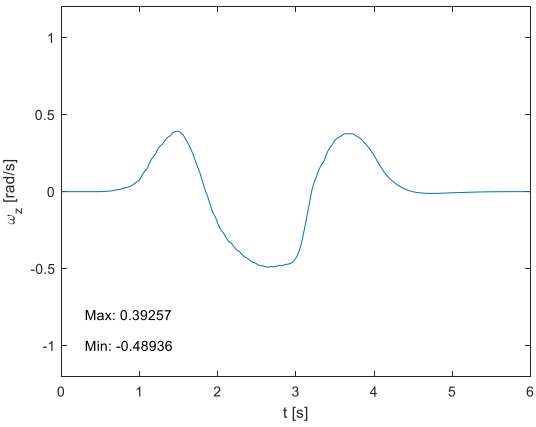

- - – desired
— – obtained
x – longitudinal vehicle position
y – lateral vehicle position
t – time
y_g – projected path deviation
α_v – steering wheel angle
a_y – lateral acceleration
ω_z – yaw rate

CONCLUSIONS

It can be concluded that the trajectories formed on the basis of Bézier curves and those formed on the basis of independent Adams Car simulations are successful in overcoming the given test tracks.

However, if the parameters of the vehicle's dynamic behavior are also taken into account (lateral acceleration and cornering speed of the vehicle), the following can be concluded:

For a test track according to ISO 3888-1:

- paths formed on the basis of Bézier curves cause lower values of acceleration and yaw rate at speeds up to 22.5 m/s,
- at speeds greater than or equal to 25 m/s, the paths formed on the basis of independent Adams Car simulations give lower values of acceleration and yaw rate.

For test track #3:

- paths formed on the basis of Bézier curves cause lower values of acceleration and yaw rate at speeds up to 15 m/s,
- at a speed of 17.5 m/s, paths formed on the basis of Bézier curves cause lower values of acceleration and yaw rate in the positive direction, while these values are lower in the negative direction for paths formed on the basis of Adams Car simulations,
- at speeds greater than or equal to 20 m/s, the paths formed on the basis of independent Adams Car simulations give lower values of acceleration and yaw rate.

For a test track according to ISO 3888-2:

- paths formed on the basis of Bézier curves cause lower values of acceleration and yaw rate at speeds up to 12.5 m/s,
- at a speed of 15 m/s, paths formed on the basis of Bézier curves cause lower values of acceleration and yaw rate in the positive direction, while these values are lower in the negative direction for paths formed on the basis of Adams Car simulations,
- at speeds greater than or equal to 17.5 m/s, the paths formed on the basis of independent Adams Car simulations give lower values of acceleration and yaw rate.

It can be concluded that paths based on Bézier curves are better chosen at lower speeds, while paths formed based on Adams Car simulations give better results at higher speeds – this is perhaps best seen in the diagram representing the vehicle path at a vehicle speed of 30 m/s with on test track #3.

The difference between the desired and obtained trajectories are minimal and allow the vehicle to pass the test track without contact with its boundaries (except in the mentioned case when the vehicle moves at a speed of 30 m/s on the test track #3 along a path formed on the basis of Bézier curves, when the model would in any case choose trajectory based on Adams Car simulation).

It should be mentioned here that the graphs of the dependence of the projected deviation from the path y_g on time are not a measure of the deviation of the actual path from the desired path and that it can best be seen from the already mentioned graphs that represent the path of the vehicle on the test tracks.

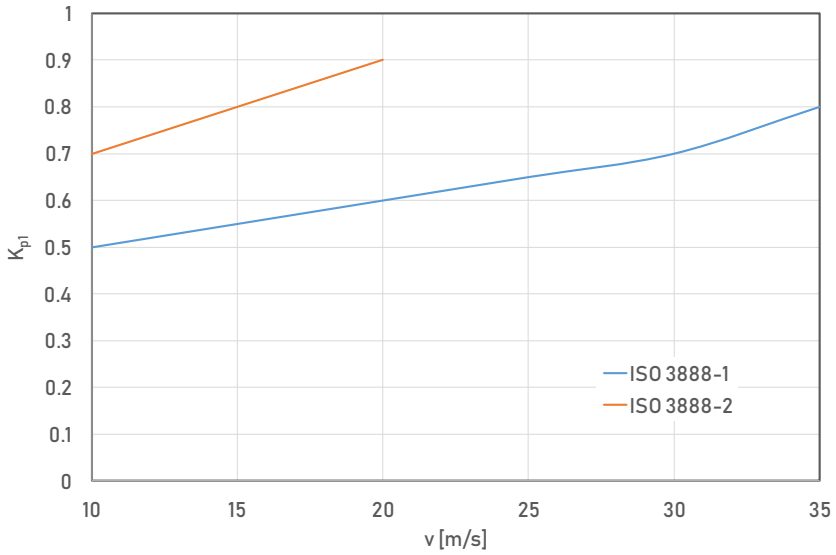

Figure 7. K_{p1} vs vehicle speed for different test tracks.

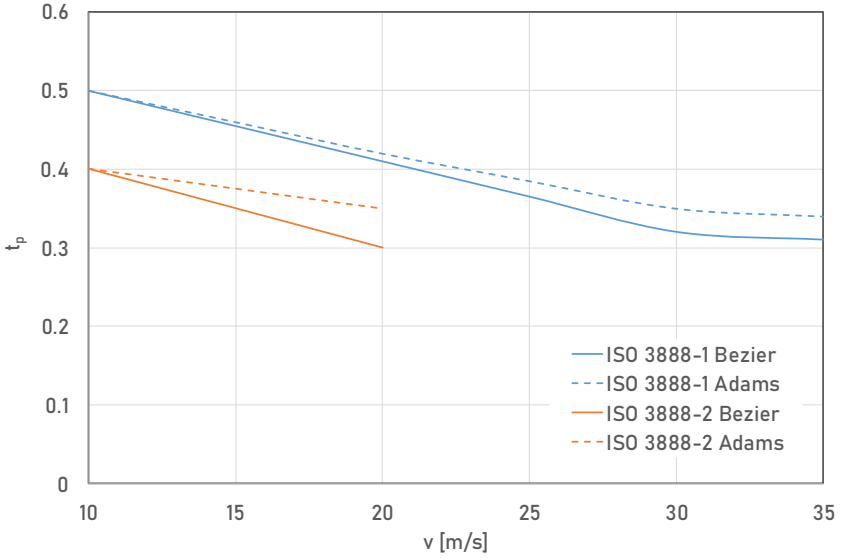

Figure 8. t_p vs vehicle speed for different test tracks.

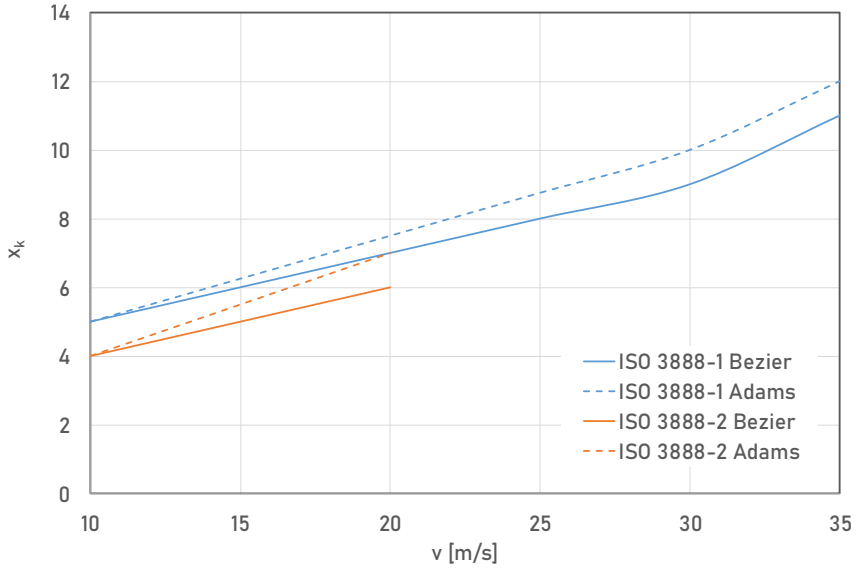

Figure 9. x_k vs vehicle speed for different test tracks.

Figures 7-9 show the dependence of the model parameters on the speed of the manoeuvre and the dimensions of the test track. The following conclusions can be drawn:

Parameter K_{p1}:

- grows with increasing speed,
- grows with the reduction of the dimensions of the test track, that is, with the sharpening of the manoeuvre,
- does not depend on the path formation method.

Parameter t_p:

- decreases with increasing speed (while the product of this value and the speed of the vehicle, which represents the distance of the forward looking point from the vehicle, increases),
- decreases with the reduction of the dimensions of the test track, that is, with the "sharpening" of the manoeuvre, in a similar way as the driver reduces the distance of the forward looking point in sharper curves,
- decreases more slowly with trajectories defined on the basis of independent Adams Car simulations compared to trajectories based on Bézier curves, which is in line with the previous statement that trajectories generated on the basis of Adams Car simulations are more favourable at higher speeds, that is, they require less sharp manoeuvres.

Parameter x_k:

- increases with speed;
- decreases with the reduction of the dimensions of the test track, that is, with the "sharpening" of the manoeuvre, similar to the parameter t_p,
- grows faster with speed for trajectories defined on the basis of independent Adams Car simulations compared to the paths based on Bézier curves, which is in accordance with what was stated for the t_p parameter.

Manoeuvres performed by the presented model do not cause lateral acceleration and yaw rate that exceed the limits of the vehicle's capabilities (at least not on surfaces with good grip). In addition to the above, the developed model causes "smooth" control of the steering wheel (which has a great influence on the above-mentioned quantities), just as a human would do, unlike some models presented in the literature.

The authors did not find in the literature models that were able to effectively perform a double lane change at the limits of the vehicle's manoeuvrability – most of the presented models were developed for changing the traffic lane on the highway with manoeuvres that are far from the limits of the vehicle's capabilities. Therefore, the authors believe that the greatest contribution of the developed model is its ability to successfully drive the vehicle through the test track, which allows the vehicle to avoid obstacles on the road ahead, at the limits of the vehicle's capabilities and the surface. In addition, the developed model is simple, computationally undemanding and easily adaptable to any vehicle.

The co-simulations carried out can serve to create a database of feasible manoeuvres, which can be used to decide on a manoeuvre – braking to a stop, braking to slow down before changing lane or just changing lane.

Future models, in order to represent an improvement of the model presented in this paper, should consider the following:

- the possibility of online path correction in the event of a sudden change in some of the dimensions of the test track or changes in adhesion conditions,
- influence of vehicle load (empty/full) on its dynamic behaviour,
- estimated adhesion coefficient, to the extent feasible,
- communication with other vehicles and/or infrastructure [24].

ACKNOWLEDGEMENT

The research presented in this article is funded by the Ministry of Science, Technological Development and Innovation of the Republic of Serbia under agreement No. 451-03-65/2024-03/200105 dated 5th February 2024.

REFERENCES

[1] Stamenković, D.; Popović, V. and Vorotović G.: *Lane detection algorithm using image processing for autonomous vehicle model*.
Euromaintenance 2016. Athens, 2016,

[2] Aiya, S.: *Bezier Curve Plotter, MATLAB Central File Exchange*.
https://www.mathworks.com/matlabcentral/fileexchange/30759-bezier-curve-plotter, accessed 4th September 2021,

[3] Stamenković, D.; Popović, V. and Blagojević, I.: *A brief review of strategies used to control an autonomous vehicle*.
2nd Maintenance Forum 2017. Bečići, 2017,

[4] Mitić, M.: *Empirical control of an intelligent mobile robot based on machine learning*. Ph.D. Thesis. In Serbian.
University of Belgrade, Faculty of Mechanical Engineering, Belgrade, 2014,

[5] Peng, T., et al.: *A new safe lane-change trajectory model and collision avoidance control method for automatic driving vehicles*.
Expert Systems with Applications **141**, No. 112953, 2020,
http://dx.doi.org/10.1016/j.eswa.2019.112953,

[6] Ozguner, U., et al.: *The OSU Demo '97 vehicle*.
In: *Proceedings of Conference on Intelligent Transportation Systems*. IEEE, Boston, pp.502-507, 1997,
http://dx.doi.org/10.1109/ITSC.1997.660525,

[7] Franke, U.; Bottiger, F.; Zomotor, Z. and Seeberger, D.: *Truck platooning in mixed traffic*.
Symposium Intelligent Vehicles '95. Detroit, 1995,

[8] Sorniotti, A.; Barber P. and De Pinto S.: *Path tracking for automated driving: A tutorial on control system formulations and ongoing research*.
In: Watzenig, D. and Horn, M., eds.: *Automated Driving*. Springer, Cham, pp.71-140, 2017,
http://dx.doi.org/10.1007/978-3-319-31895-0_5,

[9] Moon, C. and Choi, S.B.: *A driver model for vehicle lateral dynamics*.
International Journal of Vehicle Design **56**(1-4), 49-80, 2011,
http://dx.doi.org/10.1504/IJVD.2011.043258,

[10] Guo, K. and Guan, H.: *Modelling of driver/vehicle directional control system*.
Vehicle System Dynamics **22**(3-4), 141-184, 1993,
http://dx.doi.org/10.1080/00423119308969025,

[11] Zhao, P., et al.: *Design of a control system for an autonomous vehicle based on adaptive-PID*.
International Journal of Advanced Robotic Systems **9**(2), 2012,
http://dx.doi.org/10.5772/51314,

[12] Jalali, K.; Lambert, S. and McPhee, J.: *Development of a path-following and a speed control driver model for an electric vehicle*.
SAE International Journal of Passenger Cars - Electronic and Electrical Systems **5**(1), 100-113, 2012,
http://dx.doi.org/10.4271/2012-01-0250,

[13] Snider, J.M.: *Automatic Steering Methods for Autonomous Automobile Path Tracking*.
Carnegie Mellon University, Pittsburgh, 2009,

[14] Falcone, P.; Borrelli, F.; Asgari, J.; Tseng, H.E. and Hrovat, D.: *Predictive active steering control for autonomous vehicle systems*.
IEEE Transactions on Control Systems Technology **15**(3), 566-580, 2007,
http://dx.doi.org/10.1109/TCST.2007.894653,

[15] Markkula, G.; Benderius, O.; Wolff, K. and Wahde, M.: *A review of near-collision driver behavior models*.
Human Factors: The Journal of the Human Factors and Ergonomics Society **54**(6), 1117-1143, 2012, http://dx.doi.org/10.1177/0018720812448474,

[16] Zainal, Z.; Rahiman, W. and Baharom, M.N.R.: *Yaw rate and sideslip control using PID controller for double lane changing*.
Journal of Telecommunication, Electronic and Computer Engineering **9**(3-7), 99-103, 2017,

[17] Marino, R.; Scalzi, S. and Netto, M.: *Nested PID steering control for lane keeping in autonomous vehicles*.
Control Engineering Practice **19**(12), 1459-1467, 2011, http://dx.doi.org/10.1016/j.conengprac.2011.08.005,

[18] Mouri, H. and Furusho, H.: *Automatic path tracking using linear quadratic control theory*.
IEEE Conference on Intelligent Transportation Systems. Boston, 1997,

[19] Sharp, R.; Casanova, D. and Symonds, P.: *A mathematical model for driver steering control, with design, tuning and performance results*.
Vehicle System Dynamics **33**(5), 289-326, 2000, http://dx.doi.org/10.1076/0042-3114(200005)33:5;1-Q;FT289,

[20] Ziegler, J., et al.: *Making Bertha Drive - An autonomous journey on a historic route*.
IEEE Intelligent Transportation Systems Magazine **6**(2), 8-20, 2014, http://dx.doi.org/10.1109/MITS.2014.2306552,

[21] Kapania, N.R. and Gerdes, J.C.: *Design of a feedback-feedforward steering controller for accurate path tracking and stability at the limits of handling*.
Vehicle System Dynamics **53**(12), 1687-1704, 2015, http://dx.doi.org/10.1080/00423114.2015.1055279,

[22] MacAdam, C.C.: *Application of an optimal preview control for simulation of closed-loop automobile driving*.
IEEE Transactions on Systems, Man, and Cybernetics **11**(6), 393-399, 1981, http://dx.doi.org/10.1109/TSMC.1981.4308705,

[23] Isermann, R.; Schorn, M. and Stählin, U.: *Anticollision system PRORETA with automatic braking and steering*.
Vehicle System Dynamics **46**(S1), 683-694, 2008, http://dx.doi.org/10.1080/00423110802036968,

[24] Simon, J. and Mester, G.: *Critical Overview of the Cloud-Based Internet of Things Pilot Platforms for Smart Cities*.
Interdisciplinary Description of Complex Systems **16**(3-A), 397-407, 2018, http://dx.doi.org/10.7906/indecs.16.3.12.